Radiation Effects of Bombardment of Quartz and Vitreous Silica by 7.5-kev to 59-kev Positive Ions*

R. L. HINES AND R. ARNDT
Northwestern University, Evanston, Illinois

(Received December 14, 1959; revised manuscript received April 8, 1960)

Bombardment of quartz or vitreous silica by positive ions produces a surface layer of altered refractive index whose depth and refractive index is found from reflection coefficient measurements at 650 mμ, 600 mμ, 550 mμ, 500 mμ, and 450 mμ. The layer depths and the changes in refractive index versus integrated flux are given for H_2^+, D_2^+, He^+, Ne^+, A^+, Kr^+, and Xe^+ ions with energies from 7.5 kev to 59 kev. All bombardments give approximately equal changes in refractive index for a given energy input per unit volume of material as long as the ion energy is low enough so that energy loss by ionization is negligible. The changes produced by ion bombardment are attributed to direct lattice displacements and are shown to be consistent with the known changes produced in quartz and vitreous silica by fast neutron bombardment. Thermal spikes produced by knock-on atoms in quartz and vitreous silica are experimentally shown to be unimportant for knock-on energies near 45 kev.

INTRODUCTION

IN the course of an investigation[1] of the interesting observation by Koch[2] that 60-kev Kr^+ ion bombardment markedly decreased the reflection coefficient of glass for visible light, it developed that optical measurements of ion-bombarded surfaces could give useful information about radiation effects attributed to atomic displacements. First, the ion mass and energy can be controlled to reproduce exactly, if desired, the flux of knocked-on atoms produced by fast neutron or other energetic particle irradiation. Second, optical wavelengths are of the same order as the ion penetration so both the change in property of the bombarded material and the penetration depth of the ions can be found. This approach gives no direct information about the nature of the defects produced, but it is effective in determining what parameters of the energetic atoms are important in producing the observed changes.

Brooks[3] has classified the major problems in the theory of radiation effects into three categories: (1) the mechanism of damage production, (2) the nature and mobility of the imperfections produced, and (3) the effect of imperfections on measureable properties of the solid. This paper deals with the first category and in particular with the importance of cooperative effects due to the dissipation of the incident ion energy in a very small volume in the solid.

Quartz and vitreous silica were selected for the present study because their behavior under neutron irradiation has been extensively studied by Primak[4] and others.[5,6] Part of the damage observed has been attributed by Primak to the local temperature spikes produced by the dissipation of the energy of the knocked on atoms in small volumes. In ion bombardment, both the penetration and the energy of the ion are known so that the local temperature can be calculated. Alternatively, ions which liberate different amounts of energy in the same distance can be compared to show the effect of temperature spikes having different maximum temperatures but identical volumes. The present study sets an upper limit on the extent of temperature spikes produced in silica by energetic atoms in terms of experimentally measureable quantities. Thus it differs from the usual treatment of thermal spikes based on theoretical estimates of displacement production.

BEHAVIOR OF ENERGETIC ATOMS

Complete discussions of atomic displacements in energetic solids are given by Dienes and Vineyard,[7] and Seitz and Koehler[8], and the important results are restated here to clarify the relationship between ion bombardment and radiation effects in general. The initial interaction, as far as displacements are concerned, of a high-energy particle is to collide with and impart considerable energy to a lattice atom. If E and M_1 are the energy and mass of the incident particle, and M_2 is the mass of the lattice atom, the maximum energy, T_m, that can be transferred is

$$T_m = 4M_1M_2(M_1+M_2)^{-2}E. \quad (1)$$

As an example, a 0.25-Mev neutron can impart a maximum energy of 45 kev to a knock-on atom in quartz. The weighted averages of the atomic weight ($M_2=20$) and the atomic number of the atoms in SiO_2 are used here instead of calculating individually the effect of silicon and oxygen atoms.

The primary knock-on atom collides with and displaces other lattice atoms and loses energy until it has too little energy to create new displacements. Energy

* Supported by the U. S. Atomic Energy Commission.
[1] R. L. Hines, J. Appl. Phys. **28**, 587 (1957).
[2] J. Koch, Nature **164**, 19 (1949).
[3] H. Brooks, J. Appl. Phys. **30**, 1118 (1959).
[4] W. Primak, Phys. Rev. **110**, 1240 (1958).
[5] M. Wittels and F. A. Sherrill, Phys. Rev. **93**, 1117 (1954).
[6] P. G. Klemens, Phil. Mag. **1**, 938 (1956).
[7] G. J. Dienes and G. H. Vineyard, *Radiation Effects in Solids* (Interscience Publishers, Inc., New York, 1957).
[8] F. Seitz and J. S. Koehler, Solid-State Physics, edited by F. Seitz and D. Turnbull (Academic Press, Inc., New York, 1956), Vol. 2.

loss by ionization will be small as long as

$$Em/M_1<I_e/8, \tag{2}$$

where m is the electron mass and I_e is the lowest electronic excitation energy of the target material which is given by the low-energy limit of the main optical absorption band. The energies of the final knock-on atoms will be less than the energy, $E_d(\sim 25$ ev), required to produce a new additional displacement. If (2) is satisfied by the primary knock-on atom, then the total number of displacements produced per incident particle, N_d, is

$$N_d=E/2E_d. \tag{3}$$

As the displaced atoms share energy with surrounding atoms, the region will have an energy in excess of thermal energy and thus a "temperature spike" is created whose initial volume, V, is the region over which the initial displacements are distributed and whose initial temperature rise, ΔT, is given by

$$\Delta T=E/(\rho cV), \tag{4}$$

where c is specific heat and ρ the density of the material. Subsequently, the heat will be conducted away during a time dependent on the thermal diffusivity of the material. If any energy is lost by ionization, ΔT will be less than predicted by (4) because the ionized atoms dissipate their energy in electromagnetic radiation.

In the above discussion, it should be recognized that the origin of the primary energetic atom has no effect on the subsequent events as long as its energy, mass, and atomic number are specified. The exact charge state of the energetic atoms should be of minor importance in cases where the energy loss by ionization is negligible. Ion bombardments can be compared with neutron bombardments in a reactor if both are expressed in terms of the flux and energy of the primary knock-on atoms. However, reactor bombardments produce primary knock-on atoms with a wide spectrum of energies and the knock-on flux depends on the knock-on range as well as the incident neutron flux. These factors make it preferable to compare the bombardments in terms of the amount of energy, $\mathcal{E}_d$, liberated per unit volume in displacement collisions. If (2) is satisfied, then

$$\mathcal{E}_d=\tfrac{1}{2}\mathfrak{N}\int\sigma F(E_n)T_m(E_n)dE_n, \tag{5}$$

where E_n is the neutron energy, $F(E_n)$ is the energy distribution of the time-integrated neutron flux, σ is the neutron scattering cross section, and $\mathfrak{N}$ is the number of atoms per cubic centimeter. For ion bombardment, if the displacement production is uniform in the altered layer of depth, d, the energy liberated per unit volume in displacement collisions is

$$\mathcal{E}_d=FE/d, \tag{6}$$

where F is the integrated flux of ions and where it is again assumed that little of the ion energy is lost by ionization.

REFLECTION COEFFICIENT

The reflection coefficient of a surface can be analyzed to obtain information concerning the refractive index and depth of films on the surface. The numerous aspects of the theory are presented by Heavens[9] and his notation is employed here. When light is reflected at normal incidence from the interface between two nonconducting media, the reflection coefficient is

$$R_0=[(n_0-n_1)/(n_0+n_1)]^2, \tag{7}$$

where n_0 and n_1 are the refractive indices of the two media, air and quartz in this case. R_0 is defined as the ratio of reflected intensity to incident intensity. If a thin film is present on the surface, light will be reflected from both the air-film interface and the film-substrate interface and interference effects will be present. For light of wavelength λ vertically incident on a layer of thickness d_1, and refractive index n_1 which is on a substrate of index n_2, the reflection coefficient is

$$R=\frac{r_1^2+2r_1r_2\cos 2\delta_1+r_2^2}{1+2r_1r_2\cos 2\delta_1+r_1^2r_2^2}, \tag{8}$$

where $r_1=(n_0-n_1)/(n_0+n_1)$, $r_2=(n_1-n_2)/(n_1+n_2)$, and $\delta_1=2\pi n_1d_1/\lambda$. The reflection coefficient is always less than R_0, the value with no surface layer, as long as $n_1<n_2$. When $n_1=(n_2)^{\frac{1}{2}}$ and $d_1=\lambda/4n_1$, the reflective coefficient vanishes. Curve a in Fig. 1 is a typical curve of reflection coefficient versus the ratio of film depth to wavelength.

If the refractive index of the film is not uniform as a function of depth, the reflection coefficient can be derived only in special cases. However, a nonuniform film can be approximated by dividing it into several

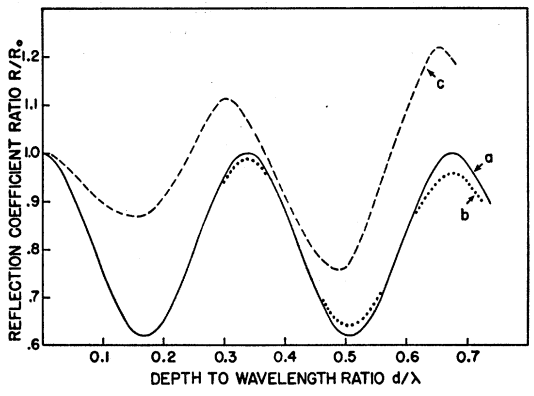

FIG. 1. Theoretical values of reflection coefficient ratio as a function of the depth to wavelength ratio for the three refractive index versus depth functions shown in Fig. 2.

[9] O. S. Heavens, *Optical Properties of Thin Solid Films* (Butterworths Scientific Publications, Ltd., London, 1955).

thinner uniform films. Two cases of interest are represented by curves b and c of refractive index versus depth shown in Fig. 2. Exact formulas are unwieldy, but if the Fresnel coefficients, r, are small compared to unity, as is the case here, a good approximation is,

$$R=|r_1+r_2e^{-2i\delta_1}+r_3e^{-2i(\delta_1+\delta_2)}|^2, \quad (9)$$

where $r_3=(n_2-n_3)/(n_2+n_3)$ and $\delta_2=2\pi n_2d_2/\lambda$. Curves b and c in Fig. 1 show the reflection coefficients for the films having the refractive index variation shown in Fig. 2.

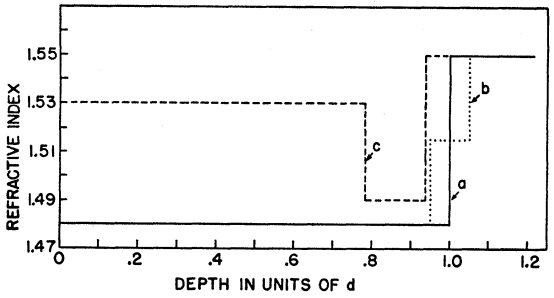

FIG. 2. Three possible forms of the variations of refractive index versus depth for ion bombarded quartz. Curves b and c coincide with a except where shown otherwise.

APPARATUS

The general layout of the bombarding system is shown in Fig. 3. The ions are created in a Phillips ionization gauge-type ion source[10] and pass through a $\frac{1}{8}$-inch diameter exit canal into the main vacuum system. The appropriate gas is bled into the ion source by means of a needle valve and the ion source pressure is adjusted for optimum operation. The energy of the emergent ions can be varied from about 1.5 kev to 11 kev. Next the ions pass through a magnetic field created by an electromagnet with 3-inch diameter pole faces, and are bent through an angle of 20°. Collimating slits in the ion beam path are set so that the intensity of impurity ions differing in mass by $\pm 15\%$ is reduced by a factor of two and those differing by $\pm 30\%$ are reduced by a factor of thirty. A retractable faraday cup is used to measure the analyzed ion beam current and is controlled by a solenoid so that the time at which it is moved out of the path of the beam can be accurately determined. When the ion current is measured a small correction, which is experimentally determined, is made for secondary electron emission.

Next, the ions pass through the main accelerating gap whose potential difference is controllable from 0 to 50 kv. The ion source voltage and the main accelerating voltage are adjusted so that ions of the desired energy are focused on the target plate in a spot about 0.5 mm in diameter. This spot is swept out into a rectangular pattern of uniform current density by electrostatic deflection plates located between the magnet and the faraday cup. Sawtooth voltage wave forms with frequencies of about 200 and 2000 cycles per second are used. A gate valve permits the samples to be changed without disturbing the main vacuum system. A hot tungsten filament is used to neutralize the charge deposited on the bombarded quartz by the ion beam.

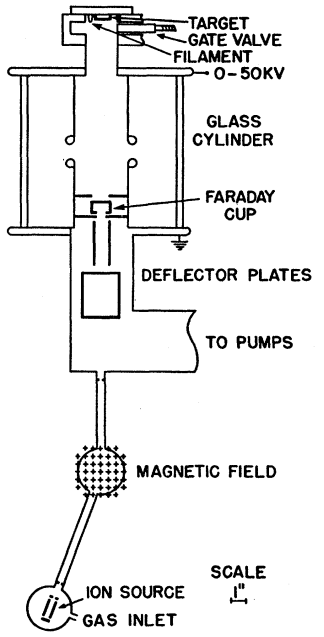

FIG. 3. Schematic layout of ion bombardment apparatus.

The ion source and magnet are adjusted with the faraday cup intercepting the beam. Then the cup is moved out of the path of the beam to allow the beam to bombard the sample. The ion current is measured again at the end of the run and usually has not changed. On long runs the ion current is checked several times. Ion beam currents range from 0.03 to 3 microamps and bombardment times range from half a second to several hours. At total ion energies below 10 kev the obtainable ion current drops rapidly which, because of contaminant film formation, prevents experiments at low energies. All bombardments are carried out at room temperature. The pressure in the region containing the sample is about 2×10^{-5} mm of Hg during bombardment. All meters are calibrated against $\frac{1}{2}\%$ laboratory standards.

The vitreous silica samples are pieces of clear fused quartz supplied by General Electric Company which are ground and polished on both sides using standard techniques. The crystalline quartz samples are cut from Brazilian rock crystal supplied by the Diamond Drill Carbon Company. All quartz samples were cut, ground, and polished so that the bombarded face was perpendicular to the optic axis as determined with polarized light. All samples were scrubbed with detergent, rinsed in distilled water and dried with a blast of clean compressed air before bombardment. The samples are about $\frac{3}{8}$-inch in diameter and about $\frac{1}{4}$ inch thick.

[10] C. F. Barnett, P. M. Stier, and G. E. Evans, Rev. Sci. Instr. 24, 394 (1953).

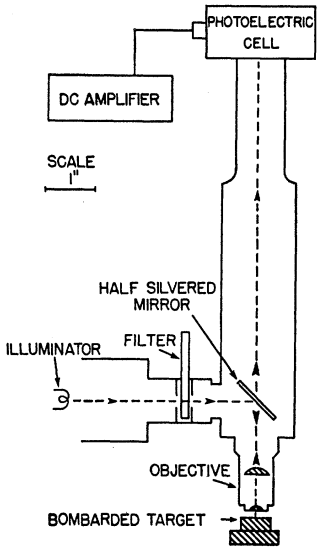

FIG. 4. Schematic layout of the vertical illumination microscope and other apparatus used to measure reflection coefficient ratios.

Since the area of the bombarded region is small, it is convenient to use the optical system of a vertical illumination microscope as shown in Fig. 4 to measure the reflection coefficient of the bombarded surfaces. A battery-powered tungsten filament lamp and a set of monochromatic filters (450 mμ, 500 mμ, 550 mμ, 600 mμ, and 650 mμ with half-widths of 18 mμ) are used for the light source. The incoming light is reflected from the half-silvered mirror in the microscope body, passes through the objective lens (0.40 N. A., 20X, 215 mm T. L.), is reflected from the surface to be measured, passes back through the objective lens, through the half-silvered mirror, and strikes a barrier layer photoelectric cell placed over the eyepiece tube. The photoelectric cell current is measured with a low impedance chopper-type dc amplifier. The light level and the amplifier impedance are low enough to assure a linear relation between light intensity and amplifier reading. The area illuminated on the sample could be varied with the microscope field adjustment from 0.07-cm diameter to 0.02-cm diameter. This method measures the reflection coefficient averaged over angles of incidence of $\pm 24°$ from normal incidence.

EXPERIMENTAL TECHNIQUE

Reflection Coefficient Measurement

Two sources of background illumination are present with the above measuring system. First, some of the light is reflected from the bottom surfaces of the bombarded sample, reenters the microscope, and strikes the photoelectric cell. By mounting the $\frac{1}{4}$-inch thick sample on a $\frac{1}{4}$-inch thick glass slide with immersion oil, much of the background is eliminated. The $\frac{1}{2}$-inch separation between the top and bottom surfaces is large enough compared to the $\frac{1}{8}$-inch working distance of the objective so that the amount of light which re-enters the microscope and strikes the photoelectric cell can be neglected. Second, some light is reflected from the lenses in the objective. The amount of background light is given by the amplifier reading when nothing is under the objective ($I_{\text{background}}$). Usually the background reading is less than 20% of the total reading over a quartz surface. The desired information is the ratio of reflection coefficients of bombarded (R) and nonbombarded (R_0) surfaces. After the sample is in position, the microscope is focused on the bombarded surface using an eyepiece. Then the eyepiece is removed and the photoelectric cell placed over the eyepiece tube. The bombarded area covers only a small portion of the sample and is easily located by moving the sample with the calibrated mechanical stage and watching the variation in reflection coefficient as indicated by the amplifier reading. The stage coordinates of the center of the bombarded area and a nonbombarded area are recorded and the sample is shifted between the two positions and the amplifier reading recorded at each position. Then the sample is moved completely out of position and the background recorded. The light source and amplifier are stable over the time (2 min) required for the measurements. The reflection coefficient ratio is calculated from the equation

$$R/R_0=(I_{\text{bombarded}}-I_{\text{background}})/(I_{\text{nonbombarded}}-I_{\text{background}}). \quad (10)$$

The entire measurement is done twice at each wavelength for each sample and the average of the two measurements is used in subsequent calculations. If the two measurements differ by more than 1% they are repeated to find the error. The final average is reproducible with an accuracy of 0.5%.

Integrated Flux Measurement

In order to plot the radiation effects as functions of integrated flux density in ions/cm^2, the flux density of the ion beam must be measured. This is done by determining the area of the bombarded spot since the ion beam current is known. Ideally, the ion beam should have a uniform current density which drops abruptly to zero at the edge of the beam. Then, if the reflection coefficient is measured as a function of position over the surface using a calibrated mechanical stage, there would be a uniform change over the bombarded area. The area could be found from the stage coordinates at which the reflection coefficient changed. Actually, the ion beam has uniform current density over a central area and then falls slowly to zero at the beam edge. The area can be measured if the reflection coefficient ratio is known as a function of the relative integrated flux density. Such a curve (see Fig. 5) is obtained by bombarding several samples with the same voltage and current settings on the bombarding apparatus but for different lengths of time. Since operating conditions are the same, the flux density profile for the ion beam will be the same in all the samples in a given series and can

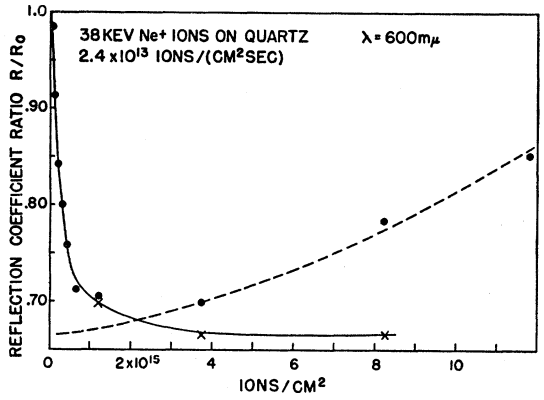

FIG. 5. The experimental points represent the combined effect of the radiation damage caused by the ions plus the effect of the contaminant film formed on the quartz surface. A theoretical curve for the reflection coefficient ratio of a saturation bombarded quartz sample with a contaminant film whose thickness is a linear function of the integrated flux is fitted to the experimental points at high fluxes (dashed curve). Extrapolation of this curve to zero flux gives the saturation value of R/R_0 due to the radiation damage alone, and the difference between the dashed curve and the saturation value of R/R_0 gives the correction for contaminant film presence. The crosses show the experimental points corrected for contaminant film presence and the solid curve gives the effect of the radiation damage alone.

be found by the procedure given below. Essentially, the method utilizes the differences in R/R_0 at various points on a sample to obtain the flux density relative to that at the center.

For a given series of bombardments which differ only in the length of bombardment time, t, the flux density in ions/(cm² sec), $j(x,y)$, is constant but depends on the coordinates x and y measured from the center of the beam. Consequently, the reflection coefficient ratio also depends on x and y as well as t. By measuring R/R_0 at all points on the bombarded area, a quantity $t'(x,y)$ can be determined experimentally by the relation

$$(R/R_0)(t,x,y)=(R/R_0)(t',0,0). \tag{11}$$

Thus $t'(x,y)$ is the time required at a flux density $j(0,0)$ to produce a value of R/R_0 equal to the value of R/R_0 observed at the point (x,y), the flux density $j(x,y)$, and the bombardment time t. The point (0,0) refers to the center of the ion beam. The right-hand side of (11) is the experimental curve of reflection coefficient ratio versus bombardment time at the center of the ion beam. Such a curve is identical to that shown in Fig. 5 except that in Fig. 5 the abscissa has been converted from time to integrated flux density.

If the changes in reflection coefficient ratio depend only on integrated ion flux density (ions/cm²), then

$$tj(x,y)=t'j(0,0) \tag{12}$$

The total ion current, i, striking the sample is known and by definition is

$$i=e\int j(x,y)dxdy \tag{13}$$

where e is the charge per ion. Eliminating $j(x,y)$ between (12) and (13) one obtains

$$j(0,0)=it\left[e\int t'(x,y)dxdy\right]^{-1} \tag{14}$$

where the integral is evaluated numerically from the experimental data. The measurement of R/R_0 at all points on the bombarded area is carried out only for one sample in each series. Once $j(0,0)$ is known, the integrated flux densities of the various bombardments are found by multiplying by the bombardment times. Best results are obtained by measuring samples which have been bombarded to give R/R_0, at the center, about 75% of the saturation value. The accuracy of the flux density measurement is estimated to be between 5% and 20% depending on the accuracy of the R/R_0 versus t curves and the magnitudes of the areas of the bombarded regions. The area of the bombarded region is defined as the total number of ions striking the sample divided by the integrated flux density at the center of the bombarded area. The areas range from 0.01 cm² to 0.1 cm².

Contaminant Film Correction

Bombardment of surfaces in a vacuum system by energetic particles usually produces a brownish-black coating on the surface.[11] This is due to the thin film of hydrocarbon molecules present on all surfaces in a vacuum system caused by exposed gaskets, wax, and diffusion pump oil. When an energetic particle strikes the film, some of the molecules polymerize to form nonvolatile substances. Since the original film of hydrocarbon molecules is continually being replaced by deposition from the vapor phase, the contaminant film continues to build up as long as the energetic particle bombardment continues. In the present case of ion bombardment, the contaminant film has a bluish-silvery appearance when viewed by reflected light, and a brownish appearance when viewed by transmitted light. Quantitatively, the contaminant film produces an increase in reflection coefficient which is superimposed on the change due to the radiation effect as shown in Fig. 5. The thickness of the film can be estimated by masking part of the bombarded area to prevent film buildup and then measuring the shift of interference fringes between the bombarded surface and a reference flat at the boundary between the masked and unmasked areas.[9] For a bombardment for which the effect of the contaminant film, R_c, is $R_c=1.2R_0$, the thickness of the film is found to be 0.009 $\pm$0.002 micron. This indicates a refractive index of about 3.0 if absorption is neglected. The absorption coefficient k per vacuum wavelength is found by measuring the decrease in transmission coefficient due to the contaminant film. For a typical sample with

[11] A. E. Ennos, Brit. J. Appl. Phys. 4, 101 (1953).

$R_c=0.5R_0$, it is found that

$$kd_c=0.0019\lambda^{-1.4}, \quad (15)$$

where d_c is the contaminant film thickness, λ the wavelength in microns, and the constant probably depends upon the conditions during film formation.

The films are very tenatious and attempts to remove them by polishing with rouge altered the bombarded quartz film before removal of the contaminant film was complete. Attempts to remove the contaminant film chemically were unsuccessful. The rate of formation of the contaminant film decreases as the current density increases, decreases as the ion mass or energy is increased, and decreases as the partial pressure of hydrocarbons in the system is decreased. The contaminant film is a severe problem in low-energy bombardments by H_2^+, D_2^+, and He^+ ions but is negligible in Kr^+ and Xe^+ bombardments at the current densities used here. In the latter case, the hydrocarbon atoms are probably sputtered off faster than they can be replenished so that the surface concentration is low.

The effect of the contaminant film on the reflection coefficient can be calculated from its refractive index, n_1, absorption, k_1, and thickness, d_1. The bombarded quartz has a refractive index $n_2=1.48$ and thickness d_2, and the substrate quartz has refractive index $n_3=1.547$. The reflection coefficient of this arrangement can be calculated in tractable form using (9). Since the contaminate film thickness is small compared to λ the expression can be expanded in terms of $(n_1d_1/\lambda)\ll 1$. In addition, it is assumed that $(k_1/n_1)\ll 1$. The final result can be identified as the individual contributions of the bombarded layer and the contaminate film, i.e.,

$$R=R_{\text{bombardment}}+R_{\text{contaminant}}, \quad (16)$$

where

$$R_c=\left[\frac{k_1}{n_1}-\left(\frac{r_3X_0+r_3r_2}{r_1X_0}\right)\sin 2\delta_2\right](4X_0r_1\delta_1)+\left(\frac{r_2}{4X_0^2r_1}\right)(4X_0r_1\delta_1)^2, \quad (17)$$

and

$$X_0=(n_0-n_2)/(n_0+n_2).$$

The quantities in large parentheses are almost independent of n_1 between $n_1=2$ and $n_1=3$ so their approximate values are found using $n_1=2.5$. The thickness, d_1, of the contaminant film in a given series of bombardments such as are shown in Fig. 5 should be proportional to the number of ions/cm^2, F, striking the sample. Then (17) can be written as

$$R_c=[k_1n_1^{-1}-0.12\sin 2\delta_2](aF/\lambda)+4.23(aF/\lambda)^2, \quad (18)$$

where $a=8\pi X_0r_1n_1d_1/F$.

The actual correction for a given series is obtained from the curves of R/R_0 versus F for each of the 5 measured wavelengths. Using overlying graphs, the experimental points for large fluxes are fitted with trial curves until the values for a and k_1/n_1 are found which give the best fit to the experimental points. These values of a and k_1/n_1 are then used to calculate the corrections at small values of integrated fluxes. The accuracy depends upon the accuracy of the R/R_0 versus F curves and the validity of the approximations made in the derivation. The total error is estimated to be $\pm 10\%$ of the value of the correction.

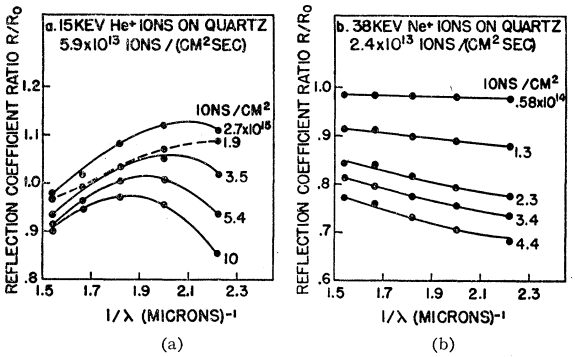

(a) (b)

FIG. 6. Experimental values of reflection coefficient ratios versus reciprocal wavelengths for 15-kev He^+ ions and 38-kev Ne^+ ions with the correction for the presence of the contaminant film included.

RESULTS

Figures 6(a) and 6(b) give the reflection coefficient as a function of reciprocal wavelength for two different bombarding conditions. Most of the results are for quartz because the changes are larger and easier to measure than those for vitreous silica. Each figure represents a series of bombardments of different time durations which give the different integrated fluxes as indicated. About ten bombardments were made in each series but it is not possible to show clearly all the information in a single figure. Most of the results can be fitted with curves of the type shown in Fig. 1(a) which then give values for the depth and refractive index of the bombarded layers. Figure 7 shows a typical

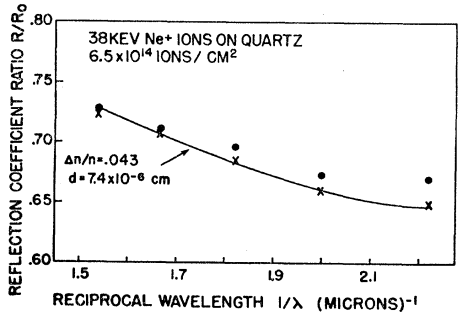

FIG. 7. The dots are the original experimental points for a typical sample, the crosses are the values after subtracting the effect of the contaminant film, and the curve gives the theoretical values for a uniform layer with the parameters shown.

case with a curve fitted to the experimental values corrected for contaminant film presence. It is recognized that the layer may be nonuniform and that (8) would not adequately predict the change in reflection coefficient. However, if the light wavelength is on the order of, or greater than, the layer thickness, the above approach may be interpreted to give an average refractive index and an effective depth for the layer. For saturation bombardments the value of $\Delta n/n$ should depend only on the properties of the bombarded solid and should be uniform as long as the depth is much larger than the distance over which the nonbombarded substrate can exert an ordering influence. Figures 8 and 9 give values of $\Delta n/n$ and d, respectively, as a function of integrated flux of 38-kev Ne^+ ions. Figure 10 gives values of $\Delta n/n$ versus integrated flux for 7.5-kev He^+ ions on vitreous silica.

All of the bombardments, except Xe^+ and Kr^+, give similar saturation type curves of $\Delta n/n$ and d versus integrated flux although the saturation value of $\Delta n/n$

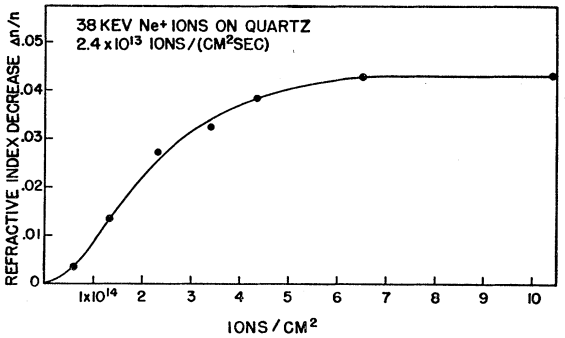

FIG. 8. The decrease in ordinary refractive index ($\lambda = 550$ mμ) of quartz as a function of integrated flux of 38-kev Ne^+ ions. The experimental values are obtained by fitting theoretical curves to the reflection coefficient ratio data shown in Fig. 6(b).

appears to depend somewhat on the penetration depth. The information can be presented adequately in terms of $F_{50}\%$ which is defined as the integrated flux which produces 50% of the saturation change in $\Delta n/n$. The layer depth, d, is taken to be the value obtained at saturation fluxes. From previous work,[1] the layer depth is believed to correspond to the range of the incident ion in most cases. However, the comparison of these experimental ranges with other experimental values and with theoretical estimates is outside the scope of this paper. All of the information obtained under different bombardment conditions is summarized in Table I in terms of the quantities defined above.

There are a number of effects of possible importance in the analysis of the results of ion bombardment of quartz but when they are considered quantitatively they turn out to be of minor importance as is shown below. One obvious effect of the ion beam will be to sputter atoms off of the quartz surface. The sputtering should be very similar to the sputtering of glass where

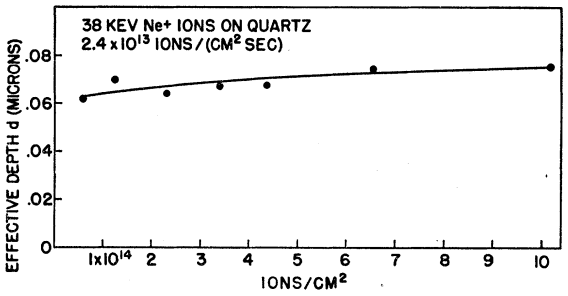

FIG. 9. Effective depth of the altered layer produced by bombardment of quartz with 38-kev Ne^+ ions as a function of integrated flux. The experimental points are obtained by fitting theoretical curves, assuming the bombarded layer has uniform optical properties, to the data shown in Fig. 6(b).

it is known that on the average a 32-kev A^+ ion sputters away 1.2 atoms from quartz.[1] Thus for a typical value for $F_{50}\%$ of 1.2×10^{14} ions/cm^2 only 1.44×10^{14} atoms/cm^2 will be sputtered away which is a layer only 0.18×10^{-8} cm thick.

The possibility that the observed decrease in reflection coefficient is not due to interference effects can be checked by measuring the increase in transmission coefficient of the bombarded surface. The absolute value of the two changes should be equal if no contaminant film is present. For a quartz sample bombarded by 47-kev A^+ ions the reflection coefficient ($\lambda = 650$ mμ) decreased in absolute value by 0.0115 ± 0.0001 and the transmission coefficient ($\lambda = 650$ mμ) increased in absolute value by 0.009 ± 0.003.[12] The transmission coefficient increase is a small change in a large number and would be difficult to measure with greater accuracy.

The changes in refractive index produced by ion bombardment are stable at room temperatures. Samples which have been remeasured after a period of six months have shown no significant changes in reflection coefficient. To investigate the stability in greater detail, samples of bombarded quartz and vitreous silica are annealed for periods of thirty minutes at successive temperatures of 100°C, 200°C, 300°C, 400°C, 500°C, 600°C, and 700°C and remeasured after each anneal. No significant changes occur until the 600°C anneal which decreases the refractive indices of both the bombarded quartz and vitreous silica to values close to that for nonbombarded vitreous silica.[12]

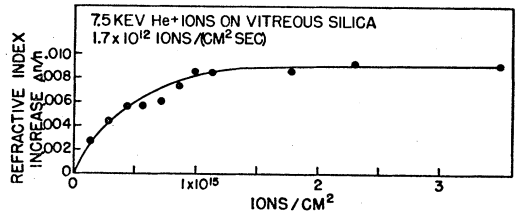

FIG. 10. The increase in refractive index of vitreous silica as a function of integrated flux of 7.5-kev He^+ ions.

[12] R. L. Hines, Bull. Am. Phys. Soc. 2, 18 (1957).

TABLE I. Summary of experimental information on ion bombardment of quartz and vitreous silica. $F_{50}\%$ is defined as the integrated flux which produces 50% of the saturation change in refractive index. The refractive index change and layer depth are found by fitting theoretical curves to the experimental values of the reflection coefficient of the bombarded surface at different wavelengths. The errors given represent the accuracy with which the theoretical curves can be fitted to the experimental values of reflection coefficient.

Ion	Ion energy E (kev)	Energy parameter Em/M_1 (ev)	Average $\Delta n/n$ at saturation	Effective layer depth (microns)	Integrated flux $F_{50}\%$ (ions/cm²)	Energy dissipation $F_{50}\%E/d$ (ev/cc)
			Quartz ($I_e/8=0.8$ ev)			
H_2^+	14.6	3.97	-0.044 ± 0.002	0.171 ± 0.009	$117.\pm19\times10^{14}$	$99.\pm10\times10^{23}$
H_2^+	19.9	5.41	-0.043 ± 0.002	0.235 ± 0.012	$406.\pm49\times10^{14}$	$359.\pm43\times10^{23}$
H_2^+	32.6	8.88	-0.051 ± 0.003	0.338 ± 0.017	$423.\pm120\times10^{14}$	$408.\pm114\times10^{23}$
D_2^+	12.8	1.74	-0.046 ± 0.005	0.219 ± 0.011	$65.\pm12\times10^{14}$	$38.0\pm7.2\times10^{23}$
D_2^+	18.8	2.55	-0.048 ± 0.002	0.290 ± 0.015	$133.\pm15\times10^{14}$	$86.2\pm10.3\times10^{23}$
D_2^+	29.6	4.02	-0.041 ± 0.002	0.400 ± 0.020	$110\pm31\times10^{14}$	$81.\pm23\times10^{23}$
He^+	7.5	1.03	-0.042 ± 0.002	0.091 ± 0.005	$17.4\pm1.2\times10^{14}$	$14.3\pm1.2\times10^{23}$
He^+	15.1	2.06	-0.042 ± 0.002	0.191 ± 0.010	$39.9\pm4.4\times10^{14}$	$31.7\pm3.5\times10^{23}$
He^+	23.5	3.22	-0.048 ± 0.002	0.272 ± 0.014	$44.5\pm4.9\times10^{14}$	$38.5\pm4.2\times10^{23}$
Ne^+	38.3	1.04	-0.043 ± 0.002	0.074 ± 0.004	$1.85\pm0.13\times10^{14}$	$9.4\pm0.8\times10^{23}$
Ne^+	43.9	1.20	-0.043 ± 0.002	0.085 ± 0.004	$2.20\pm0.15\times10^{14}$	$11.3\pm1.0\times10^{23}$
Ne^+	51.8	1.42	-0.041 ± 0.002	0.095 ± 0.005	$1.68\pm0.12\times10^{14}$	$8.1\pm0.7\times10^{23}$
A^+	22.9	0.32	-0.038 ± 0.002	0.060 ± 0.003	$2.0\pm0.4\times10^{14}$	$7.8\pm1.6\times10^{23}$
A^+	38.4	0.52	-0.040 ± 0.002	0.070 ± 0.003	$1.20\pm0.13\times10^{14}$	$6.7\pm0.8\times10^{23}$
A^+	59.0	0.80	-0.042 ± 0.002	0.100 ± 0.005	$1.50\pm0.14\times10^{14}$	$8.8\pm1.0\times10^{23}$
Kr^+	20.3	0.13	-0.029 ± 0.003	0.050 ± 0.005	$4.2\pm4.2\times10^{14}$	$17.\pm17\times10^{23}$
Kr^+	39.7	0.26	-0.034 ± 0.002	0.060 ± 0.006	$1.48\pm0.45\times10^{14}$	$9.8\pm3.0\times10^{23}$
Kr^+	59.0	0.39	-0.038 ± 0.002	0.067 ± 0.004	$0.62\pm0.06\times10^{14}$	$5.5\pm0.7\times10^{23}$
Xe^+	20.3	0.08	-0.015 ± 0.004	0.047 ± 0.010	$1.87\pm0.20\times10^{14}$	$8.3\pm1.9\times10^{23}$
Xe^+	39.4	0.16	-0.025 ± 0.002	0.053 ± 0.005	$0.81\pm0.09\times10^{14}$	$6.0\pm0.8\times10^{23}$
Xe^+	59.0	0.24	-0.032 ± 0.002	0.058 ± 0.006	$0.80\pm0.09\times10^{14}$	$8.1\pm1.1\times10^{23}$
			Vitreous silica ($I_e/8=0.8$ ev)			
He^+	7.5	1.03	$+0.009\pm0.001$	0.091 ± 0.005	$3.20\pm0.26\times10^{14}$	$2.64\pm0.25\times10^{23}$
Ne^+	38.3	1.04	$+0.011\pm0.001$	0.074 ± 0.004	$0.24\pm0.12\times10^{14}$	$1.25\pm0.62\times10^{23}$

Microscopic heating of the bombarded surface due to the energy input of the ion beam is known to be negligible under the present bombardment conditions.[1] The total energy input is low (50 milliwatts or less) and the energy is spread over a large enough area so that the temperature rise is always less than a few degrees centigrade.

The last side effect considered here is the importance of the bombarding atoms which are probably retained in the quartz as impurity atoms. This does not appear significant because the concentration reached in these bombardments is small. For 40-kev Ne^+ ions, a bombardment of $F_{50}\%$ gives an atomic concentration of 0.04% if the atoms are spread uniformly throughout the bombarded layer.

DISCUSSION

The light ion bombardments H_2^+, D_2^+, and He^+ produce quite similar effects. The molecular ions will be disassociated, as they enter the solid, by collisions and the energy will be shared equally between the two incident atoms. Thus the penetration of an 8-kev D^+ ion should be the same as that found for a 16-kev D_2^+ ion. The reflection coefficient measurements show definite evidence of nonuniformity in the film because of the large penetration depth of the ions. At low integrated fluxes the maximum reflection coefficient is well above unity and generally resembles Fig. 1(c) which is due to a layer of low refractive index below the surface. This agrees with the picture that as the ions penetrate, they lose energy and at lower energies $(dE/dx)_{\text{displacements}}$ probably increases. Thus the rate of damage is higher beneath the surface and a subsurface layer of low refractive index would be formed before the surface layer is appreciably altered. At large fluxes the curves resemble Fig. 1(b). Saturation damage has been produced at all depths except the extreme limit of ion penetration. There the damage is less because relatively few ions have penetrated so that the refractive index versus depth is similar to Fig. 2(b). The average refractive index is found by assuming that (8) will be valid near a minimum in the reflection curve. The uncertainty in the analysis of the nonuniform layers causes most of the large errors quoted for $F_{50}\%$.

The medium weight ions Ne^+ and A^+ have much smaller penetrations and consequently show no evidence of nonuniform layers. The Ne^+ bombardments in particular should closely duplicate the knock-on atoms formed in quartz because the atomic number and mass of Ne is the weighted average of those for Si and O.

Bombardments by the heavy ions Kr^+ and Xe^+ are difficult to interpret because the absolute change in reflection coefficient is smaller than for the other ions and consequently the accuracy of determination of d and $\Delta n/n$ is less than for the other ion bombardments. Also, there is evidence that the damage continues to change slowly after a rapid initial change (Fig. 11). The layer depth continues to increase (Fig. 12) after the change in refractive index has saturated (Fig. 13). A possible interpretation is that the knock-on atoms

produced by the Xe^+ and Kr^+ ions would have a greater penetration than the Xe^+ and Kr^+ ions themselves. From (1) it is seen that the maximum energy of a knock-on atom produced in quartz by a 59-kev Kr^+ ion is 37 kev. But referring to the data for penetration of Ne^+ ions in quartz, such a knock-on atom would have a penetration in excess of the depth of the layer produced by low flux Kr^+ bombardments. Thus the initial rapid rise may be attributed to the penetration of the Xe^+ ions and the subsequent slower rise attributed to the penetration of the high-energy knock-on atoms produced by the Xe^+ ions. Experiments at high energies would clarify this concept because the layers would be thicker and greater accuracy could be obtained for the refractive index and depth.

In comparing these results with previous results reported for ion bombardment of glass, it is evident that a different mechanism must be involved because $F_{50\%}$ for 33.5-kev A^+ ions on glass is 1.5×10^{16} ions/cm^2 but for quartz $F_{50\%}$ for 38.4-kev A^+ ions is 1.2×10^{14} ions/cm^2. Furthermore, glass is a disordered structure and should resemble fused quartz in its behavior. However, bombardment of fused quartz increases the refractive index whereas bombardment of glass decreases the refractive index. Consequently, it now appears that the changes observed in glass must be related to the constituents other than SiO_2 which are present in glass. In particular sodium ions are present and are known to diffuse through glass. The bombardment probably greatly increases the diffusion rate and sputters the sodium atoms off the surface[13] so that in effect it etches out the sodium and leaves a layer of vitreous silica.

The changes in refractive index produced by ion bombardment agree in most respects with those observed by Primak[4] for neutron bombarded quartz. For 50% of the saturation change in refractive index, Primak finds that an integrated neutron flux $\int F_n dE$ of 8.4×10^{19} n/cm^2 is required where the flux responsible for the damage has an energy spectrum proportional to $1/E$ from 0.01 to 1 Mev. From (5), this gives a value of $\mathcal{E}_d=4.0\times10^{23}$ ev/cc which produces 50% of the saturation change in refractive index. The primary knock-on flux ($M_{av}=20$, $N_{av}=10$) will have all energies up to 180 kev but with the above energy distribution, the average knock-on energy, weighted according to the amount of damage a particular knock-on will produce, is 45 kev. By comparison, a 45-kev neon bombardment ($M=20$, $N=10$) gives from (6) a value of $\mathcal{E}_d=11\times10^{23}$ ev/cc for the flux which produces 50% of the saturation change in refractive index. This is considered reasonable agreement in view of the difficulty of measuring the neutron flux responsible for the observed changes in quartz.

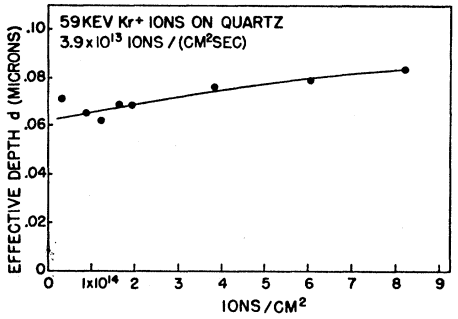

FIG. 12. Effective depth of the layer produced when quartz is bombarded by 59-kev Kr^+ ions. The increase in depth for fluxes larger than that required for saturation (see Fig. 13) is attributed to the penetration of the high-energy knock-ons produced by the Kr^+ ions.

The shape of the curves of refractive index versus flux is the same for both neutron irradiation and ion bombardment. However, the absolute change in refractive index of ion bombarded quartz ($\Delta n=0.067\pm0.002$) is significantly less than that observed for neutron irradiated quartz ($\Delta n=0.077$). This may be due to the ordering effect of the undamaged quartz substrate present in ion bombardment. As can be seen from Table I, the saturation change in $\Delta n/n$ decreases for small bombarded layer depths. Also, when the bombarded quartz is annealed, the refractive index decreased to the value for nonbombarded vitreous silica. Evidently annealing reduces the ordering effect of the nonbombarded substrate and permits all of the bom-

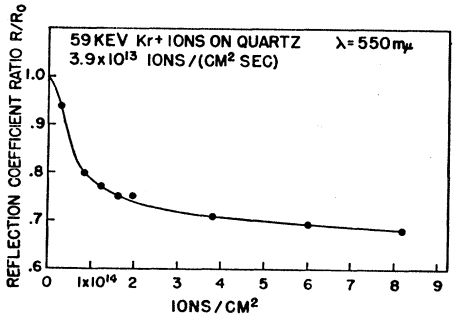

FIG. 11. Reflection coefficient ratios ($\lambda=550$ mμ) versus integrated flux for quartz bombarded by 59-kev Kr^+ ions.

[13] L. Holland, Brit. J. Appl. Phys. **9**, 410 (1958).

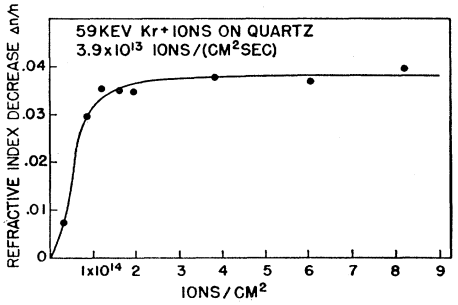

FIG. 13. Decrease in ordinary refractive index of quartz bombarded by 59-kev Kr^+ ions. The experimental points are obtained by fitting theoretical curves to the data shown in Fig. 11.

barded quartz to achieve the saturation disordered state.

The importance of the local heating produced by the individual ions can be assessed in two ways. First, the local temperature after all displacements have occured can be estimated if the displacements are assumed to be distributed uniformly within a sphere whose diameter is equal to the depth of the damaged layer. From (3) it is calculated that about 900 displacements are created by a 45-kev Ne atom. These are spread out in a cascade pattern with considerable scattering starting at the entry point, so a spherical approximation for the energy distribution is probably good. From (4) and the experimental layer depth of 8.5×10^{-6} cm, the local temperature rise is estimated to be 8.4°C for the temperature spike produced by a 45-kev Ne^+ ion. This temperature is far too low to produce any of the observed changes since phase transitions in quartz require temperatures of 1000°C or more. Thus Ne^+, or silica knock-on atoms, in silica in the energy range of 45 kev and probably higher as well, spread their energy over large volumes and hence cannot produce significant temperature changes. Although the temperature rise at lower energies is not directly known, it can be estimated from the available information. It is seen that the data presented here for Ne^+ ions agree with the linear relation between ion penetration and energy predicted by Nielsen.[14] Assuming such a linear relation, if the measured altered layer depths are extrapolated to lower Ne^+ ion energies, the temperature rise will increase inversely as the square of the ion energy. In particular, a 3.4-kev Ne^+ ion, or silica knock-on, would increase the local temperature to the melting point of quartz (~1500°C) over a spherical region containing 1×10^4 atoms. From the criterion (2) it is seen that 45-kev Ne^+ ions, or silica knock-ons, may lose part of their energy by ionization. This will make the actual temperature rise lower than that calculated from (4). Likewise, the temperature rise extrapolated to lower ion energies may be less than that given if some energy is lost by ionization. However, it must be remembered that the criterion (2) is an order of magnitude estimate and that the energy loss by ionization may still be small for the Ne^+ energies given here. Since the energy per unit volume ($F_{50\%}E/R$ in Table I) of Ne^+ ions required to produce 50% of the damage is only 20% more than that required of A^+, Kr^+, and Xe^+ ions, which do satisfy the criterion (2), it appears that most of the energy of 38-kev to 52-kev Ne^+ ions is dissipated in displacement production. In view of the lack of quantitative verification of the criterion (2), the results presented here are best regarded as an upper limit for the temperature rise produced by a given Ne^+ ion or silica knock-on. Or, alternatively, local temperatures on the order of the melting point of quartz (~1500°C) will be created by Ne^+ ions, or silica knock-ons, only for energies below 3.4 kev and will involve the heavier masses. In view of the low local temperatures produced, the decrease in $F_{50\%}E/d$ is probably due to changes in the amount of energy lost by ionization for the different masses.

The above observations suggest that the changes in refractive index of bombarded quartz must be due to the independent contributions of knock-ons. Since the effect of temperature spikes is doubtful, the changes are thought to be due to displacements alone with little or no contributions from temperature spikes. From (3) and the experimentally known layer depth, it is calculated that the probability that a given atom has been displaced after an integrated flux of $F_{50\%}$ is 30%. The saturation concentration of interstitials and vacancies is certainly much smaller than 30% so most of the primary defects will have annealed out. Because of the local strain created by interstitials and vacancies and the nature of the SiO_2 molecular bonds, the lattice at the site of an interstitial or vacancy probably does not return to its initial configuration when the defect is annealed if the interstitial and vacancy concentration is large. Thus a disordered structure gradually builds up and saturation would be expected for fluxes which give on the order of 100% probability for displacement of a given atom.

For vitreous silica, a different mechanism must be present because for $F_{50\%}$ the displacement probability of a given atom is only 7% (7.5-kev He^+ bombardment) and the final state is known to be denser than the initial state. The bombardment may enable the vitreous silica to reach a more ordered and consequently more dense state than is otherwise possible. In the formation of vitreous silica, as it is cooled from the melt, the rate of ordering will become negligible at temperatures well above room temperature. Thus the order present at room temperature is usually that which would be present in thermodynamic equilibrium at much higher temperatures. The bombardment may increase the ordering rate and permit the vitreous silica to achieve a greater degree of order. This effect is well known in studies of the ordering of $AuCu_3$ by electron irradiation.[14]

CONCLUSIONS

The changes in reflection coefficient for visible light which are observed when quartz and vitreous silica are bombarded by ions of mass numbers from 1 to 131 and energies from 7.5 kev to 60 kev are due to formation of surface layers of altered refractive index. The layer depth depends on the energy and mass of the bombarding ions. The changes in refractive index are attributed to the atomic displacements created by the incident ions and are in agreement with the changes observed in fast neutron irradiated quartz and vitreous silica. Ions of all the masses and energies employed produce equal amounts of damage in terms of energy expended

[14] R. A. Dugdale, *Report of the Bristol Conference on Defects in Crystalline Solids* (The Physical Society, London, 1955).

per unit volume of bombarded material as long as the energy parameter of the incident ions is low enough so that energy loss by displacement production predominates. From calculations of the local temperatures produced by the ions and comparison between ions having different energies but similar penetrations, it appears that the effect of temperature spikes is unimportant for knock-on atoms in silica with energies near 45 kev.

ACKNOWLEDGMENTS

The authors are indebted to H. W. Paik for his assistance in making many of the measurements, to B. Lunde for her help in the early stages of the experiment, and to A. W. Ewald for several helpful comments.

PHYSICAL REVIEW VOLUME 119, NUMBER 2 JULY 15, 1960

Fundamental Lattice Dispersion Frequencies of NaCl and KCl at 82°K

MARVIN HASS
U. S. Naval Research Laboratory, Washington, D. C.
(Received February 17, 1960)

The infrared dispersion frequencies of NaCl and KCl at 82°K were measured by infrared absorption of thin films and were found to be 170±2 cm^{-1} and 149±2 cm^{-1}, respectively. These values can be compared with those predicted by formulas of Szigeti, Odelevski, Lundqvist, and others relating the dispersion frequency to the elastic and dielectric constants. Good agreement seems to be obtained using the Szigeti formula or a combination of the Lundqvist and Odelevski formulas at low temperatures where anharmonic effects are small.

I. INTRODUCTION

IN this note experimental values of the fundamental infrared dispersion frequencies of NaCl and KCl at 82°K are reported. Measurements at these low temperatures enable anharmonic effects to be accounted for in a more satisfactory manner. This is important when comparing observed frequencies and those calculated using a formula derived independently by Szigeti[1] and Odelevski[2] which expresses the infrared dispersion frequency in terms of the elastic and dielectric constants. When room-temperature values of these constants are inserted, some deviations are found to occur. These may be attributed partly to anharmonic effects and partly to the simple model used in the derivation of the formula. By comparing observed frequencies at low temperatures with calculated frequencies using low-temperature dielectric and elastic constants, the nature of the deviations may be clarified. Attempts to explain part of the deviations in terms of a more complicated model of dielectric polarization have been made recently by Dick and Overhauser[3] and by Hanlon and Lawson[4] in connection with the related problem of the effective charge. A treatment assuming a more complicated potential involving three-body as well as two-body interactions has been discussed by Lundqvist.[5] The frequencies calculated using these various proposed formulas will be given after the experimental data is presented.

II. EXPERIMENTAL

These studies were carried out using a Perkin-Elmer Model 12 monochromator modified for grating operation as suggested by Lord and McCubbin.[6] A grating ruled at the University of Michigan with 320 lines per inch was employed. The resolution was about 3 cm^{-1}. The entire optical system was enclosed in a plastic film housing in which air was recirculated through a molecular sieve desiccant in order to reduce the intense water-vapor absorption.

The dispersion frequency was determined by measuring the frequency of maximum absorption of films of NaCl and KCl less than one micron thick which were vacuum evaporated onto quartz plates 0.58 mm thick. These quartz plates were cemented with General Electric 7031 varnish to the sample holder of a metal transmission Dewar having polythene windows. The sample holder was surrounded with a radiation shield. The temperature was measured in a separate experiment using a copper-constantan thermocouple soldered to a sheet of copper which was cemented to a piece of quartz in the sample position. The temperature measured in this manner was 82°K.

The data is shown in Table I along with Barnes and

[1] B. Szigeti, Proc. Roy. Soc. (London) **A204**, 51 (1950). See also M. Born and K. Huang, *Dynamical Theory of Crystal Lattices* (Oxford University Press, New York, 1954), p. 111, for further discussion.
[2] V. I. Odelevski, Izvest. Akad. Nauk S.S.S.R. Ser. Fiz. **14**, 232 (1950).
[3] B. G. Dick, Jr., and A. W. Overhauser, Phys. Rev. **112**, 90 (1958).
[4] J. E. Hanlon and A. W. Lawson, Phys. Rev. **113**, 472 (1959).
[5] S. O. Lundqvist, Arkiv Fysik **9**, 435 (1955); Arkiv Fysik **12**, 263 (1957).
[6] R. C. Lord and T. K. McCubbin, Jr., J. Opt. Soc. Am. **47**, 689 (1957).